JB
Journals.ASM.org

Unveiling Unusual Features of Formation of Septal Partition and Constriction in Mycobacteria—an Ultrastructural Study

Srinivasan Vijay, Deepak Anand, and Parthasarathi Ajitkumar

Department of Microbiology and Cell Biology, Indian Institute of Science, Bangalore, Karnataka, India

The ultrastructural functions of the electron-dense glycopeptidolipid-containing outermost layer (OL), the arabinogalactan-mycolic acid-containing electron-transparent layer (ETL), and the electron-dense peptidoglycan layer (PGL) of the mycobacterial cell wall in septal growth and constriction are not clear. Therefore, using transmission electron microscopy, we studied the participation of the three layers in septal growth and constriction in the fast-growing saprophytic species *Mycobacterium smegmatis* and the slow-growing pathogenic species *Mycobacterium xenopi* and *Mycobacterium tuberculosis* in order to document the processes in a comprehensive and comparative manner and to find out whether the processes are conserved across different mycobacterial species. A complete septal partition is formed first by the fresh synthesis of the septal PGL (S-PGL) and septal ETL (S-ETL) from the envelope PGL (E-PGL) in *M. smegmatis* and *M. xenopi*. The S-ETL is not continuous with the envelope ETL (E-ETL) due to the presence of the E-PGL between them. The E-PGL disappears, and the S-ETL becomes continuous with the E-ETL, when the OL begins to grow and invaginate into the S-ETL for constriction. However, in *M. tuberculosis*, the S-PGL and S-ETL grow from the E-PGL and E-ETL, respectively, without a separation between the E-ETL and S-ETL by the E-PGL, in contrast to the process in *M. smegmatis* and *M. xenopi*. Subsequent growth and invagination of the OL into the S-ETL of the septal partition initiates and completes septal constriction in *M. tuberculosis*. A model for the conserved sequential process of mycobacterial septation, in which the formation of a complete septal partition is followed by constriction, is presented. The probable physiological significance of the process is discussed. The ultrastructural features of septation and constriction in mycobacteria are unusually different from those in the well-studied organisms *Escherichia coli* and *Bacillus subtilis*.

The presence of a bilayered plasma membrane and a triple-layered cell wall, constituted by an electron-dense outermost layer (OL) containing mostly glycopeptidolipids (11, 37), an electron-transparent layer (ETL) below, consisting of an arabinogalactan-mycolic acid complex (22, 36), and an electron-dense peptidoglycan layer (PGL), has been observed and characterized through ultrastructural and biochemical studies in *Mycobacterium smegmatis* (7, 12, 16, 27), *Mycobacterium xenopi* and other mycobacterial species (reviewed in references 2, 17, 24, and 27), *Mycobacterium tuberculosis* (3, 9, 33; reviewed in reference 5), *Mycobacterium leprae* (33), and *Mycobacterium kansasii* (25, 27). Numerous studies had been carried out on the ultrastructures of the OL, ETL, and PGL, their molecular compositions, and the probable roles of these layers in the physiology, pathology, and virulence of different mycobacterial species (6–8; reviewed in references 3 and 5). However, the functional roles of these layers in cell division remained unclear. Studies on mycobacterial cell division (reviewed in reference 14) using transmission electron microscopy (TEM) for *Mycobacterium lepraemurium* (18), *M. leprae* (10, 15), *Mycobacterium avium* (26), and *M. vaccae* (32) showed the formation of a complete septal partition during cell division, followed by constriction to generate two daughter cells. Transmission and scanning electron microscopic studies on *Mycobacterium vaccae* (32) and *M. tuberculosis* (9) cells, and fluorescence microscopic studies on *M. smegmatis* and *M. tuberculosis* (34), showed the presence of low proportions of "V"-shaped cells during the final stages of division. Similar "V"-shaped cells had been observed previously for *Arthrobacter atrocyaneus* (31) and *Arthrobacter crystallopoietes* (20), but in higher proportions. The "V"-shaped cells were found to undergo division at the connecting point through the rupture of outer layers to generate daughter cells.

Although the morphological aspects of the formation of a septal partition, constriction, and physical separation of daughter cells have been examined, the ultrastructural aspects of the participation of the OL, ETL, and PGL in the formation of the septal partition and constriction during cell division remain to be understood. Therefore, in the present study, a comprehensive and comparative ultrastructural analysis was performed in order to find out how and in what sequence the OL, ETL, and PGL participate in the formation of a septal partition and in constriction in mycobacteria. The fast-growing saprophytic species *M. smegmatis*, the slow-growing opportunistic human pathogen *M. xenopi*, and the slow-growing human pathogen *M. tuberculosis* were chosen as the experimental systems. The present study essentially involved confirmation of the consistent and reproducible presence of the OL, ETL, and PGL in the sections of *M. smegmatis*, *M. xenopi*, and *M. tuberculosis* samples, as described by others (3, 5, 7, 12, 27, 33). Subsequently, detailed documentation and cross-comparisons were carried out on the mode and sequence of participation of the OL, ETL, and PGL in septal partition formation and constriction events in the three species in order to find out whether these processes are conserved across different mycobacterial species. Models were proposed for these events in *M. smegmatis* and *M. xenopi*, in comparison to the deviations in *M. tuberculosis*. Finally, striking differences in septal partition and

Received 15 September 2011 **Accepted** 9 November 2011
Published ahead of print 18 November 2011
Address correspondence to Parthasarathi Ajitkumar, ajit@mcbl.iisc.ernet.in.
Supplemental material for this article may be found at http://jb.asm.org/.

doi:10.1128/JB.06184-11

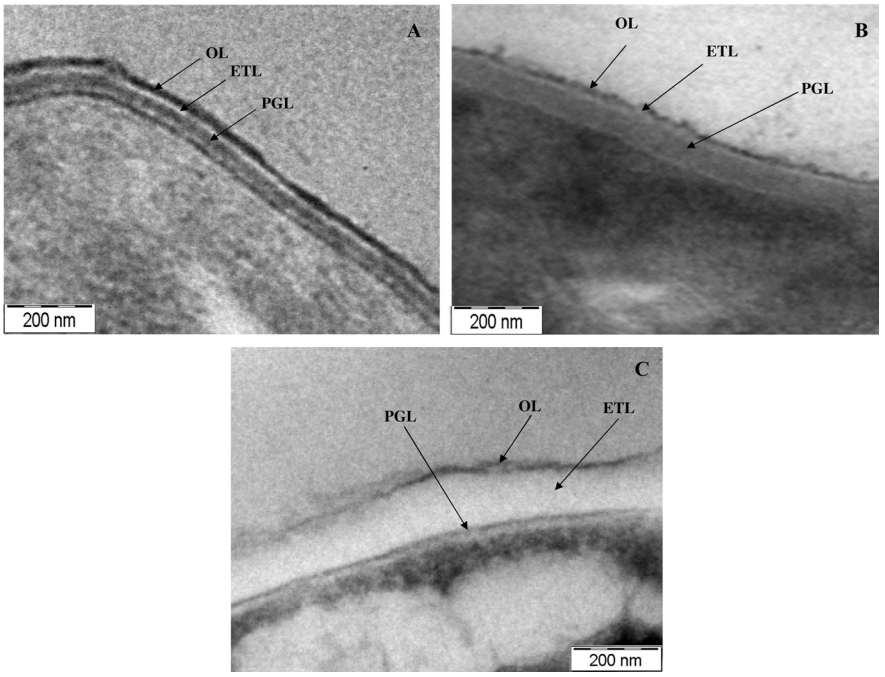

FIG 1 Ultrastructures of cell envelopes of *M. smegmatis* (A), *M. xenopi* (B), and *M. tuberculosis* (C). OL, outer layer; ETL, electron-transparent layer; PGL, peptidoglycan layer.

constriction between mycobacteria, on the one hand, and *Escherichia coli* and *Bacillus subtilis*, on the other, were shown.

MATERIALS AND METHODS

Bacterial strains and growth conditions. *M. smegmatis* mc^{2}155 (from William Jacobs), *M. xenopi*, and *M. tuberculosis* H_{37}Ra (National JALMA Institute of Leprosy and Other Mycobacterial Diseases, Agra, India) cells were grown to an optical density at 600 nm (OD_{600}) of 0.6 (mid-log phase) in Middlebrook 7H9 broth with albumin-dextrose-catalase (ADC) supplement in the presence or absence of 0.05% Tween 80 at 37°C and 170 rpm.

TEM. *M. smegmatis*, *M. xenopi*, and *M. tuberculosis* cells were processed for transmission electron microscopy (TEM) as described previ-

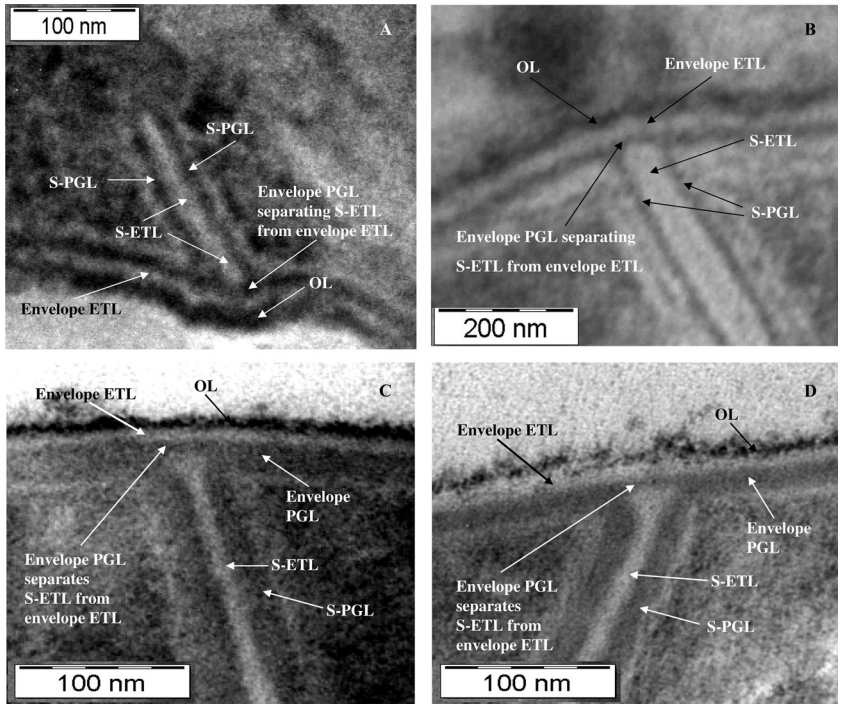

FIG 2 Ultrastructural profile of the initial stages of formation of the septal partition in *M. smegmatis* (A and B) and *M. xenopi* (C and D). The S-PGL and S-ETL grow from the E-PGL. The S-PGL is connected to the E-PGL, but the S-ETL is separated from the E-ETL by the presence of the E-PGL. The S-ETL is flanked by the S-PGL (one layer on each side).

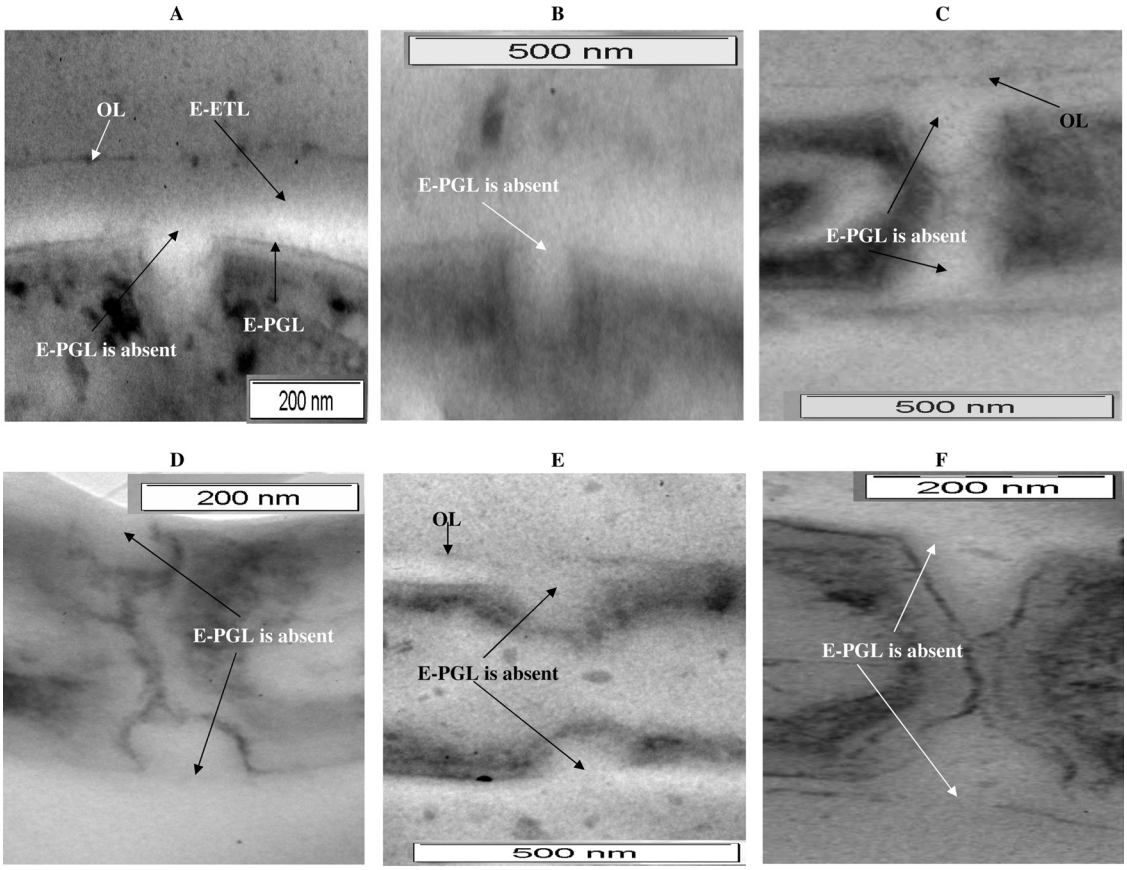

FIG 3 Images of initial stages of formation of the septal partition in *M. tuberculosis* cells. The S-PGL and S-ETL grow continuously with the E-PGL and E-ETL, respectively. The E-PGL is not present between the S-ETL and E-ETL. Note that in the very early stage of the initiation of septal partition, the S-PGL and S-ETL grow continuously with, and connected to, the E-PGL and E-ETL, respectively (A).

ously (32). In brief, the cells were fixed in 1% (vol/vol) osmium tetroxide buffered with 0.15 M cacodylate buffer (pH 7.2) for 1 h at room temperature, washed once with the same buffer, and postfixed for 2 h at room temperature in 0.15 M cacodylate buffer (pH 7.2) containing 2% (wt/vol) tannic acid (to stain the outermost layer, with background staining with lead citrate) and 2% (vol/vol) glutaraldehyde. The cells were then washed once with the buffer, refixed in 1% (vol/vol) osmium tetroxide overnight at 4°C, dehydrated in a graded series of ethanol, and embedded in LR White resin. Ultrathin sections were stained with 0.5% uranyl acetate and 0.04% lead citrate and were observed under a JEOL-100 CX II electron microscope at 80 kV.

RESULTS AND DISCUSSION

Ultrastructural features of the OL, ETL, and PGL in *M. smegmatis*, *M. xenopi*, and *M. tuberculosis*. To begin the study, the consistently reproducible and distinct presence of the OL, ETL, and PGL of the mycobacterial cell envelope was ascertained in the *M. smegmatis*, *M. xenopi*, and *M. tuberculosis* TEM samples (100 septating cells of each species) (Fig. 1A, B, and C, respectively). The ultrastructural profile of the triple layers remained unaltered in cells cultured in the presence or absence of Tween 80 (data not shown), indicating that the observations reported in this study were not influenced by culture conditions. *M. leprae* from mouse lymph node and other infected tissues (10, 15), *M. avium* grown in Middlebrook and Cohn 7H9 medium with Tween 80 (26), and *M. vaccae* grown in heart infusion broth (32) also showed the same profile of a triple-layered cell wall, irrespective of different culture conditions. The transmission electron micrographs in Fig. 1 confirmed previous observations on the ultrastructural features of the triple layers of *M. smegmatis* (7, 12, 27), *M. xenopi* (27), and *M. tuberculosis* (3, 5, 33). Recently, cryoelectron tomography (CET) (16) and cryoelectron microscopy of vitreous sections (CEMOVIS) (37) have revealed that the OL of mycobacteria consists of two layers, instead of the one layer revealed by conventional TEM. However, the topologies of the PGL and ETL/electron-transparent zone (ETZ), which were revealed by conventional TEM, have not yet been clearly assigned using the CET or CEMOVIS method. Further, the presence of glycopeptidolipids in the OL (outer membrane) had been demonstrated by both conventional TEM (11) and CEMOVIS (37). Thus, studies using the CET (16) and CEMOVIS (37) methods have supported and/or added more detail to the ultrastructural features of the mycobacterial cell envelope revealed by conventional TEM.

Ultrastructure of septal-partition formation and constriction in *M. smegmatis*, *M. xenopi*, and *M. tuberculosis*. In order to differentiate the roles of the PGL and ETL of the septum from those of the PGL and ETL already existing in the envelope, it was necessary to distinguish between them. Therefore, the PGL and ETL of the freshly synthesized septum were called the septal PGL (S-PGL) and septal ETL (S-ETL), respectively. Similarly, the envelope PGL and ETL were called the E-PGL and E-ETL, respec-

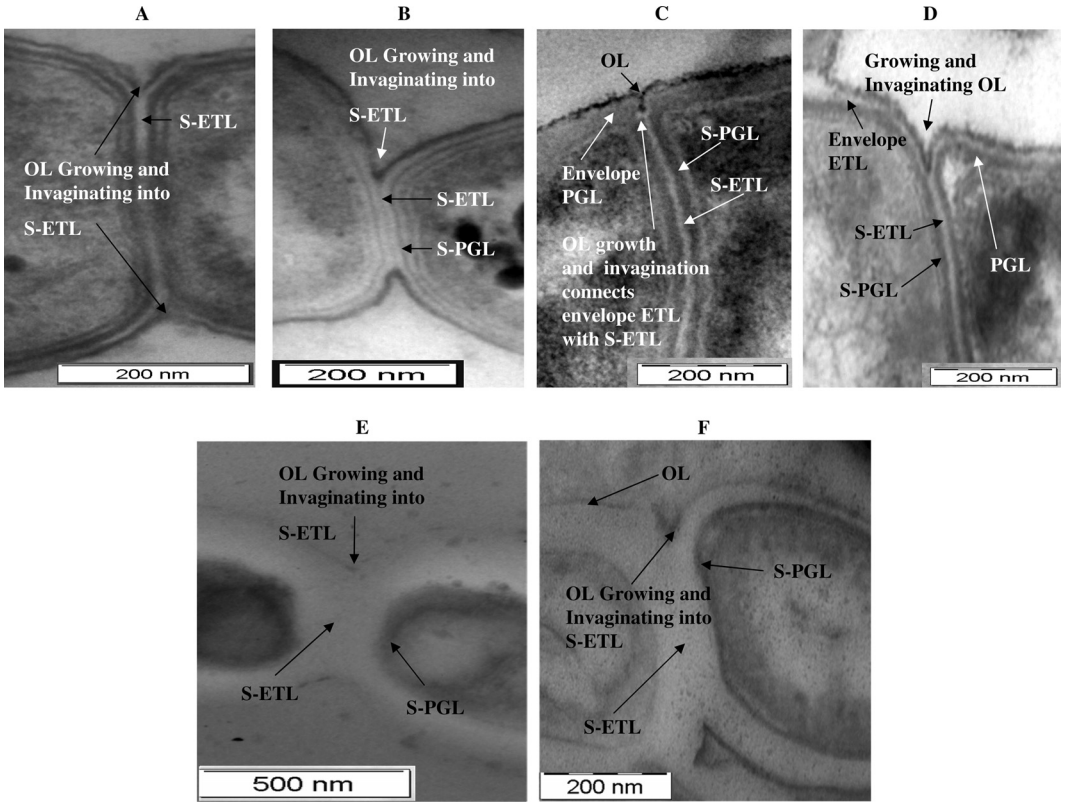

FIG 4 Ultrastructural features of the initiation of constriction. (A, C, and E) The OL begins to grow and invaginate into the S-ETL in *M. smegmatis*, *M. xenopi*, and *M. tuberculosis*, respectively. The E-PGL separates the S-ETL from the E-ETL during septation in *M. smegmatis* and *M. xenopi*. This separation disappears when the OL invaginates into the S-ETL. This makes the E-ETL continuous with the S-ETL. In contrast, no such temporary separation of the S-ETL from the E-ETL by the E-PGL seems to occur in *M. tuberculosis*. The S-ETL is flanked by the S-PGL (one layer on each side). (B, D, and F) Later stages of growth and invagination of the OL into the septal ETL in *M. smegmatis*, *M. xenopi*, and *M. tuberculosis*, respectively.

tively. In septating *M. smegmatis* (Fig. 2A and B) and *M. xenopi* (Fig. 2C and D) cells ($n = 100$), both the S-PGL and S-ETL were found to grow from the E-PGL, but without the growth or invagination of the E-PGL. Although the S-PGL was connected to the E-PGL, the S-ETL was not continuous with the E-ETL, due to the presence of the E-PGL between the S-ETL and E-ETL in all the samples examined (Fig. 2). Examination of more septum initiation images of *M. smegmatis* and *M. xenopi* clearly showed that the S-ETL is separated from the E-ETL by the E-PGL in both *M. smegmatis* and *M. xenopi* (see Fig. S1A to D and E to H, respectively, in the supplemental material). However, in *M. tuberculosis*, the E-PGL was not present between the E-ETL and S-ETL, and therefore, there was no partitioning of the S-ETL from the E-ETL in any of the samples (50 early septating cells) (Fig. 3). Even images of very early initiation of septation in *M. tuberculosis* showed the absence of the E-PGL between the S-ETL and E-ETL (Fig. 3A and B), in contrast to the pattern in *M. smegmatis* and *M. xenopi*. The presence of a thick E-ETL, which is characteristic of *M. tuberculosis*, may be noted in these images. Thus, the growth of the S-PGL and S-ETL was continuous with that of the E-PGL and E-ETL, respectively (Fig. 3). The S-PGL and S-ETL grew in parallel, with the S-PGL flanking the S-ETL, and progressed to completion to generate a complete septal partition in *M. smegmatis*, *M. xenopi*, and *M. tuberculosis* cells (see the top, center, and bottom panels, respectively, of Fig. S2 in the supplemental material). The septal partition in *M. tuberculosis* cells was found to be much wider than those in *M. smegmatis* and *M. xenopi* cells. Only subsequent to the formation of a complete septal partition was septal constriction initiated by the growth and invagination of the OL into the S-ETL of the septal partition in *M. smegmatis*, *M. xenopi*, and *M. tuberculosis* cells (Fig. 4A, C, and E, respectively). In *M. smegmatis* and *M. xenopi* cells, with the growth and invagination of the OL into the S-ETL, the E-PGL, which separated the S-ETL from the E-ETL, disappeared, and the S-ETL became continuous with the E-ETL (Fig. 4A and C, respectively). Septal constriction progressed further toward division in *M. smegmatis*, *M. xenopi*, and *M. tuberculosis* cells (Fig. 4B, D, and F, respectively). Because an ultrastructural profile, and not a molecular profile, of septation was the focus of the study, the locations of mycobacterial cell division proteins in these cells were not determined.

Similarities and differences in septal-partition formation and constriction. The data in the present study demonstrate that the ultrastructural features of the mode and sequence of participation of the OL, ETL, and PGL in the formation of a septal partition and constriction are similar in *M. smegmatis*, *M. xenopi*, and *M. tuberculosis* cells. Further, straight, diagonal, or curved septal partition could be observed across the length of the septating cells in all three species (see Fig. S2 in the supplemental material). As in these three species, the formation of a complete septal partition, either straight, diagonal, or curved, prior to constriction had been observed in cell division studies on *M. lepraemurium* (18), *M. smegmatis* (1), *M. leprae* (10, 33), *M. vaccae* (32), *M. avium* (26),

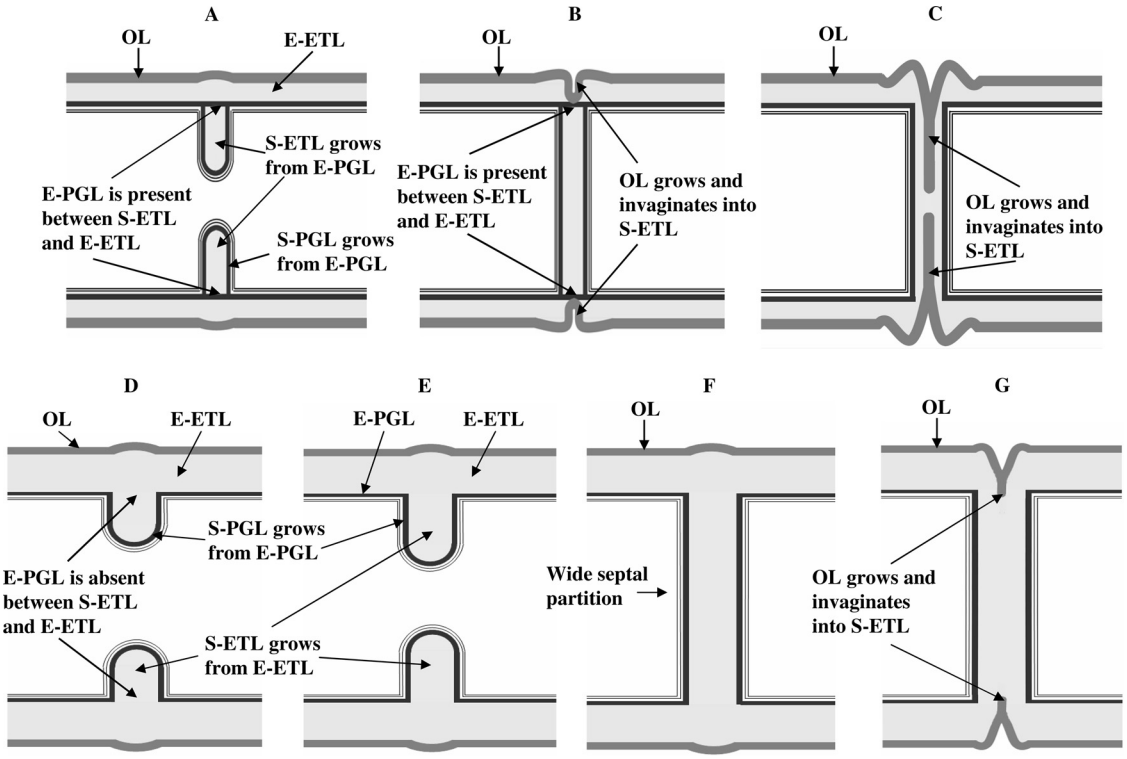

FIG 5 Model for formation of the septal partition and constriction in *M. smegmatis*, *M. xenopi*, and *M. tuberculosis*. (A to C) *M. smegmatis* and *M. xenopi*. (A) The S-ETL and S-PGL grow, connected to the E-PGL, which separates the S-ETL from the E-ETL. (B) Completion of formation of the septal partition constituted by the S-ETL and S-PGL. The continued presence of the E-PGL, separating the S-ETL from the E-ETL, is shown. The OL starts to grow and invaginate into the S-ETL to form constriction. (C) Progression of growth and invagination of the OL into the S-ETL. (D to G) *M. tuberculosis*. (D) The S-ETL and S-PGL grow continuously with the E-ETL and E-PGL, respectively. In contrast to the process in *M. smegmatis* and *M. xenopi*, the E-PGL is not present between the S-ETL and E-ETL. (F) Completion of formation of septal partition. (G) The OL begins to grow and invaginate into the S-ETL to form constriction.

and several other mycobacterial species (19). Similarly, septal constriction was also initiated by the OL in an identical manner, by growing and invaginating into the S-ETL, in all three species. In spite of such conservation of ultrastructural features of septal-partition formation and constriction across a large number of mycobacterial species, some specific differences could be observed between *M. tuberculosis* and *M. smegmatis*/*M. xenopi* cells. One of the notable differences was that the E-PGL, which formed a partition between the S-ETL and the E-ETL in *M. smegmatis* and *M. xenopi* cells, and persisted until the formation of a complete septal partition and the initiation of constriction, was absent in *M. tuberculosis* cells (compare Fig. 2 with Fig. 3). Another was that, in contrast to the circumferential constriction in *M. smegmatis* and *M. tuberculosis* cells, constriction in *M. xenopi* always occurred only from one plane of the septating cell (see Fig. S3 in the supplemental material; compare Fig. S3A to C [*M. xenopi*] with D to F [*M. smegmatis*] and G [*M. tuberculosis*]). This kind of constriction from one plane of septating *M. xenopi* cells may help the formation of "V"-shaped cells during the end stage of septation. The formation of "V"-shaped cells in the "snapping postfission" mode of cell division has been observed in low proportions in *M. vaccae* (32), *M. smegmatis* (34), and *M. tuberculosis* (9, 34) and in higher proportions in *Arthrobacter atrocyaneus* (31) and *Arthrobacter crystallopoietes* (20). In fact, we observed low proportions of "V"-shaped *M. smegmatis*, *M. xenopi*, and *M. tuberculosis* cells undergoing the "snapping mode" of cell separation (see Fig. S4A and B, C and D, and E, respectively, in the supplemental material).

Model for mycobacterial septal-partition formation and constriction. Taking into consideration the close similarities between the ultrastructural features of formation of the septal partition and constriction in *M. smegmatis* and *M. xenopi*, and the difference observed with *M. tuberculosis*, models for the processes in *M. smegmatis* and *M. xenopi* cells (Fig. 5A to C) and in *M. tuberculosis* cells (Fig. 5D to G) are proposed. The formation of a complete septal partition prior to the initiation of constriction in this model is consistent with the observations made in studies of cell division in *M. leprae* (10), *M. avium* (26), and *M. vaccae* (32). It is noteworthy that these features are strikingly absent in the ultrastructural profile of septation in *Escherichia coli* (4) and *Bacillus subtilis* (28), where no complete septal partition is ever formed and septal growth and constriction occur together (see Fig. S5A and B, respectively, in the supplemental material). Since our study was focused on the participation of triple layers in septal partition and constriction, and not on the rupture of the outer layer during the physical separation of cells, the "snapping postfission" mode of division was not incorporated in the model.

Physiological significance of the unusual mode of mycobacterial septation. The observations made in the present study on *M. smegmatis*, *M. xenopi*, and *M. tuberculosis* cells, and analyses of data from earlier studies of cell division in other mycobacteria (18), *M. leprae* (10, 15), *M. avium* (26), and *M. vaccae* (32), warrant discussion of the probable physiological significance of the unusual ultrastructural features of septal-partition formation and constriction in mycobacteria. The formation of a complete septal

partition prior to constriction and the protection of the site of septal partition by the OL until the complete formation of the partition may confer an evolutionary advantage on mycobacteria, probably due to two conditions. First, unlike *E. coli* and *B. subtilis*, which grow and divide in about 20 min, mycobacterial species grow slowly. While *M. xenopi* divides once in 24 h (30), *M. tuberculosis* divides once in 18 h *in vivo* (23), and *M. leprae* divides once in 13.5 days (21). Even the so-called "fast-growing" species *M. smegmatis* takes about 3 h to divide once (13). Second, pathogenic species, such as *M. xenopi* (29), *Mycobacterium ulcerans* (35), *M. tuberculosis*, and *M. leprae*, and nonpathogenic environmental species, such as *M. smegmatis*, need to survive under adverse conditions in the host system or in the environment. Therefore, the covering of the region of septation by the OL and the holding of two daughter cells together by parental cell envelope layers may give the required strength to the formative nascent polar regions of daughter cells and protect them against adverse environmental conditions during long periods of septation and division.

ACKNOWLEDGMENTS

This work was supported by part-grants from the DBT Centre of Excellence in Tuberculosis and from DBT–IPSBBR/Pathogen Biology and by infrastructure support from the DST-FIST and the UGC Centre for Advanced Study. S.V. was a CSIR Senior Research Fellow.

The technical advice of S. S. Indi and the technical help of P. V. Balasubramaniam in TEM are acknowledged.

REFERENCES

1. **Barksdale L, Kim K-S.** 1977. *Mycobacterium*. Bacteriol. Rev. **41**:217–372.
2. **Brennan PJ, Nikaido H.** 1995. The envelope of mycobacteria. Annu. Rev. Biochem. **64**:29–63.
3. **Brennan PJ.** 2003. Structure, function, and biogenesis of the cell wall of *Mycobacterium tuberculosis.* Tuberculosis **83**:91–97.
4. **Conti SF, Gettner EM.** 1962. Electron microscopy of cellular division in *Escherichia coli.* J. Bacteriol. **83**:544–550.
5. **Crick DC, Quadri L, Brennan PJ.** 2008. Biochemistry of the cell envelope of *Mycobacterium tuberculosis*, p 1–19. *In* Kaufmann SHE, Rubin E (ed), Handbook of tuberculosis: molecular biology and biochemistry. Wiley-VCH Verlag GmbH & Co KGaA, Weinheim, Germany.
6. **Daffé M, Draper P.** 1998. The envelope layers of mycobacteria with reference to their pathogenicity. Adv. Microb. Physiol. **39**:131–203.
7. **Daffé M, Dupont MA, Gas N.** 1989. The cell envelope of *Mycobacterium smegmatis*: cytochemistry and architectural implications. FEMS Microbiol. Lett. **61**:89–94.
8. **Daffé M, Etienne G.** 1999. The capsule of *Mycobacterium tuberculosis* and its implications for pathogenicity. Tuber. Lung Dis. **79**:153–169.
9. **Dahl JL.** 2004. Electron microscopy analysis of *Mycobacterium tuberculosis* cell division. FEMS Microbiol. Lett. **240**:15–20.
10. **Edwards RP.** 1970. Electron-microscope illustrations of division in *Mycobacterium leprae.* J. Med. Microbiol. **3**:493–499.
11. **Etienne G, et al.** 2002. The impact of the absence of glycopeptidolipids on the ultrastructure, cell surface and cell wall properties, and phagocytosis of *Mycobacterium smegmatis.* Microbiology **148**:3089–3100.
12. **Etienne G, et al.** 2005. The cell envelope structure and properties of *Mycobacterium smegmatis* mc^2155: is there a clue for the unique transformability of the strain? Microbiology **151**:2075–2086.
13. **Gadagkar R, Gopinathan KP.** 1980. Growth of *Mycobacterium smegmatis* in minimal and complete media. J. Biosci. **2**:337–348.
14. **Hett EC, Rubin EJ.** 2008. Bacterial growth and cell division: a mycobacterial perspective. Microbiol. Mol. Biol. Rev. **72**:126–156.
15. **Hirata T.** 1978. Electron microscopic observations of cell division in *Mycobacterium leprae* by means of serial ultrathin sectioning. Int. J. Lepr. Other Mycobact. Dis. **46**:160–166.
16. **Hoffmann C, Leis A, Niederweis M, Plitzko JM, Engelhardt H.** 2008. Disclosure of the mycobacterial outer membrane: cryo-electron tomography and vitreous sections reveal the lipid bilayer structure. Proc. Natl. Acad. Sci. U. S. A. **105**:3963–3967.
17. **Imaeda T, Kanetsuna F, Galindo B.** 1968. Ultrastructure of cell walls of genus *Mycobacterium.* J. Ultrastruct. Res. **25**:46–63.
18. **Imaeda T, Ogura M.** 1963. Formation of intracytoplasmic membrane system of mycobacteria related to cell division. J. Bacteriol. **85**:150–163.
19. **Kolbel HK.** 1984. Electron microscopy, p 249–300. *In* Kubica GP, Wayne LG (ed), The mycobacteria: a sourcebook, part A. Microbiology series, vol 15. Marcel Dekker, Inc, New York, NY.
20. **Krulwich AT, Pate LJ.** 1971. Ultrastructural explanation for snapping postfission movements in *Arthrobacter crystallopoietes.* J. Bacteriol. **105**: 408–412.
21. **Levy L.** 1970. Death of *Mycobacterium leprae* in mice and the additional effect of dapsone administration. Proc. Soc. Exp. Biol. Med. **135**:745–749.
22. **Mdluli K, Swanson J, Fischer E, Lee RE, Barry CE, III.** 1998. Mechanisms involved in the intrinsic isoniazid resistance of *Mycobacterium avium.* Mol. Microbiol. **27**:1223–1233.
23. **Patterson RJ, Youmans GP.** 1970. Multiplication of *Mycobacterium tuberculosis* within normal and "immune" mouse macrophages cultivated with and without streptomycin. Infect. Immun. **1**:30–40.
24. **Paul TR, Beveridge TJ.** 1992. Reevaluation of envelope profiles and cytoplasmic ultrastructure of mycobacteria processed by conventional embedding and freeze-substitution protocols. J. Bacteriol. **174**:6508–6517.
25. **Paul TR, Beveridge TJ.** 1994. Preservation of surface lipids and determination of ultrastructure of *Mycobacterium kansasii* by freeze-substitution. Infect. Immun. **62**:1542–1550.
26. **Rastogi N, David HL.** 1981. Growth and cell division of *Mycobacterium avium.* J. Gen. Microbiol. **126**:77–84.
27. **Rastogi N, Frehel C, David HL.** 1986. Triple-layered structure of mycobacterial cell wall: evidence for the existence of a polysaccharide-rich outer layer in 18 mycobacterial species. Curr. Microbiol. **13**:237–242.
28. **Reeve JN, Mendelson NH.** 1972. Cell morphology of *Bacillus subtilis*: the effect of genetic background on the expression of a rod-gene. Mol. Gen. Genet. **119**:11–26.
29. **Satyanarayana G, Heysell SK, Scully KW, Houpt ER.** 2011. Mycobacterial infections in a large Virginia hospital, 2001–2009. BMC Infect. Dis. **11**:113. doi:10.1186/1471-2334-11-113.
30. **Schwabacher H.** 1959. A strain of *Mycobacterium* isolated from skin lesions of a cold-blooded animal, *Xenopus laevis*, and its relation to atypical acid-fast bacilli occurring in man. J. Hyg. (Lond.) **57**:57–67.
31. **Starr MP, Kuhn DA.** 1962. On the origin of V-forms in *Arthrobacter atrocyaneus.* Arch. Mikrobiol. **42**:289–298.
32. **Takade A, Takeya K, Taniguchi H, Mizuguchi Y.** 1983. Electron microscopic observations of cell division in *Mycobacterium vaccae* V 1. J. Gen. Microbiol. **129**:2315–2320.
33. **Takade A, et al.** 2003. Comparative studies of the cell structures of *Mycobacterium leprae* and *M. tuberculosis* using the electron microscopy freeze-substitution technique. Microbiol. Immunol. **47**:265–270.
34. **Thanky NR, Young DB, Robertson BD.** 2007. Unusual features of the cell cycle in mycobacteria: polar-restricted growth and the snapping-model of cell division. Tuberculosis **87**:231–236.
35. **Tolhurst JC, Buckle G, Wellington NA.** 1959. The experimental infection of calves with *Mycobacterium ulcerans.* J. Hyg. (Lond.) **57**:47–56.
36. **Wang L, Slayden RA, Barry CE, III, Liu J.** 2000. Cell wall structure of a mutant of *Mycobacterium smegmatis* defective in the biosynthesis of mycolic acids. J. Biol. Chem. **275**:7224–7229.
37. **Zuber B, et al.** 2008. Direct visualization of the outer membrane of *Mycobacteria* and *Corynebacteria* in their native state. J. Bacteriol. **190**: 5672–5680.